Acid-Sensitive Molecular Glasses as Removable Thin-Film Protective Layers

Yu-Jin Choi, ¹ Samuel J. Warnock, ¹ Nima Alizadeh, ¹ Phong H. Nguyen, ² Dimagi Kottage, ³ Oluwadamilola Phillips, ⁴ Zhengtao Chen, ⁴ Michael L. Chabinyc, ¹ and Christopher M. Bates*, ^{1,2,3}

¹Materials Department, University of California, Santa Barbara, CA, 93106, USA
²Department of Chemical Engineering, University of California, Santa Barbara, CA, 93106, USA

³Department of Chemistry & Biochemistry, University of California, Santa Barbara, CA, 93106, USA

⁴Lam Research Corporation, Fremont, CA, 94538, USA

*E-mail: cbates@ucsb.edu

Keywords: molecular glass, protective layer, acid-labile groups, oxidation resistance

Abstract

A common problem encountered in semiconductor processing is the oxidation of metals, for example, copper interconnects that constitute a significant portion of integrated circuits. Undesired oxidation may be mitigated by the application of a protective coating at various stages of processing, the removal of which is ultimately necessary but often nontrivial. To address this challenge, here we demonstrate that acid-labile molecular glasses are both efficient at protecting copper surfaces from oxidation and readily removed after use. As evidenced by X-ray photoelectron spectroscopy, thin films of molecular glasses deposited on copper prevent underlying surface oxidation for at least 120 hours. Molecular glasses that incorporate imine groups were found to be the most acid sensitive, with a hydrophobic-to-hydrophilic solubility switch reminiscent of photoresists that is readily tunable by changing the number of imines per molecule. The exquisite acid sensitivity of these imine-based molecular glasses provides a mechanism to fully remove the protecting layer in a solution of dilute sulfuric acid as low as 1 volume percent. In summary, these results highlight the potential utility of readily accessible and tunable molecular glasses in the design of processes for fabricating advanced semiconductor devices.

Introduction

Metals—a common and useful class of materials—are unfortunately susceptible to oxidation, which causes major issues across many applications and industries. Selected examples include the erosion of infrastructure, contamination of water, and decreased performance in electronics.^{1–4} Often, undesired oxidation can be mitigated with protective coatings that prevent metals from reacting with their surroundings.^{5,6} Efforts towards developing novel protective coatings are extensive and typically revolve around tuning properties of relevance in specific applications. For example, the increasing demand of batteries has led to the development of coatings for lithium anodes that suppress dendrite growth.^{7,8} In this and other contexts, many chemically inert materials have been investigated, including modified nanoparticles,^{9,10} polymers,^{11–13} and composites.^{14,15}

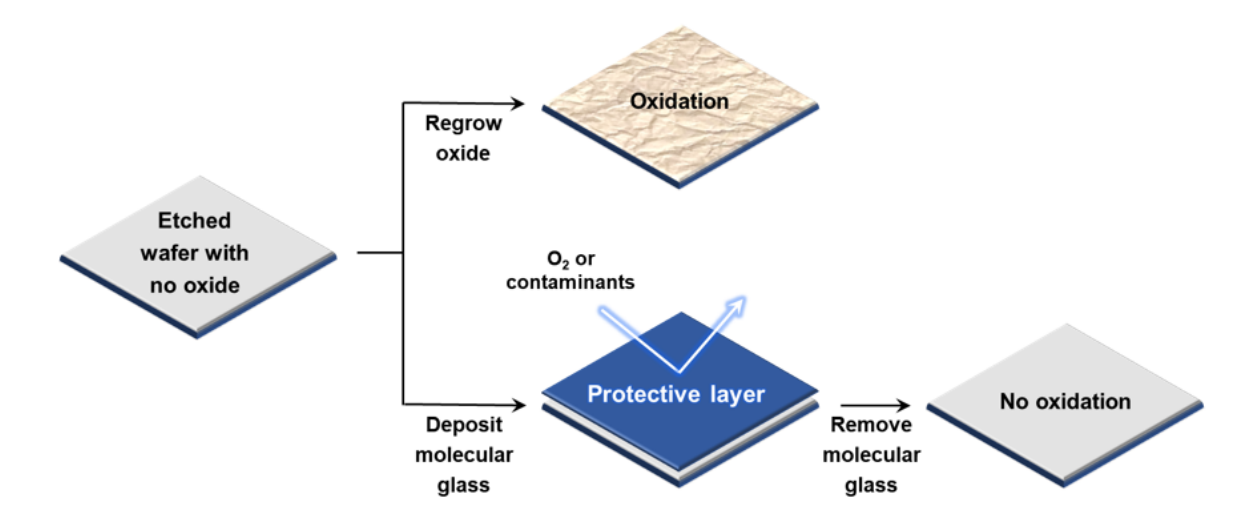
In particular, the semiconductor industry requires a wide range of protective coatings ¹⁶ because producing computer chips and memory involves hundreds if not thousands of sensitive processing steps. There are, in general, at least two desirable traits for these protective layers: they should be (1) easily applied, *e.g.* by spin coating or vapor deposition, and (2) easily removed, preferably under mild conditions. The combination of both properties enables use without damaging the underlying device at a given stage of fabrication. In the context of lithography, an important target is copper (Cu)—a common interconnect material due to its high electrical conductivity (\sim 6.0 \times 10⁷ Ω m⁻¹) and low cost—because it is readily oxidized, even at low temperatures. ^{17,18} Past work has investigated various protective layers for Cu, including alkanethiolate monolayers, ^{19,20} metal alloys, ²¹ and graphene, ¹ as well as small molecules consisting of nitrogen and sulfur heteroatoms with aromatic groups in Cu-dispersed solutions. ²²⁻²⁴ However, a significant challenge in using these materials in the semiconductor industry resides in the inherent tradeoff between stability and processability. While stability is

required for a good protective layer, highly stable materials are often difficult to deposit and/or remove from the substrate. Returning to graphene, although it is indeed an effective protective coating,²⁵ application requires vapor deposition with custom equipment and removal is nontrivial under mild conditions.

An appealing solution to this challenge may lie in the design of molecular glasses non-crystalline (organic) small molecules that lack long-range order due to local packing constraints. The amorphous and low-molecular-weight nature of molecular glasses makes them easy to apply by spin-coating or vapor deposition with standard industry equipment.²⁶ Moreover, in analogy to the amorphous polymers used extensively as photoresists in semiconductor fabs, molecular glasses form uniform and isotropic thin films, ²⁷ which is highly beneficial for protective coatings since defects such as grain boundaries²⁸ are susceptible to oxidation and other chemical attack.²⁹ Equally important, several well-established design strategies can be leveraged from the fields of drug delivery, 30 organic electronics, 31,32 and highresolution photoresists^{33,34} to prevent crystallization in molecular glasses, including: (1) nonplanarity that disfavors close/regular molecular contact, e.g. skewed aromatic groups, (2) loworder point-group symmetry to slow crystallization, 35 and (3) a lack of strong intermolecular interactions. 36-38 When properly designed, molecular glasses can achieve remarkable kinetic stability and high densities³⁹ that are correlated with decreased gas permeability, ⁴⁰ suggesting opportunities to use them as oxidation-resistant protective layers in semiconductor unit processes.

Here, we report the synthesis and characterization of acid-sensitive molecular glasses that were designed to (i) form uniform films, (ii) slow the oxidation of metal surfaces, and (iii) be readily removed in mild acidic solutions (see Scheme 1). These materials consist of a bulky aromatic core (to inhibit crystallization) that is functionalized with acid-labile imine groups

through a one-step, catalyst-free reaction with simple purification in high yield. 41,42 (Figure 1a). Imine hydrolysis provides a convenient mechanism to switch solubility from hydrophobic (when protected) to hydrophilic (when deprotected) upon exposure to dilute solutions of sulfuric acid as low as 1 vol%, facilitating on-demand removal after use. Imine-containing molecular glasses are also efficient surface-protecting layers that can prevent the oxidation of copper substrates for at least 120 hours. In summary, our results highlight the potential of molecular glasses to serve as protective coatings in lithographic applications.



Scheme 1. Molecular glasses act as protective layers that prevent the oxidation of underlying substrates.

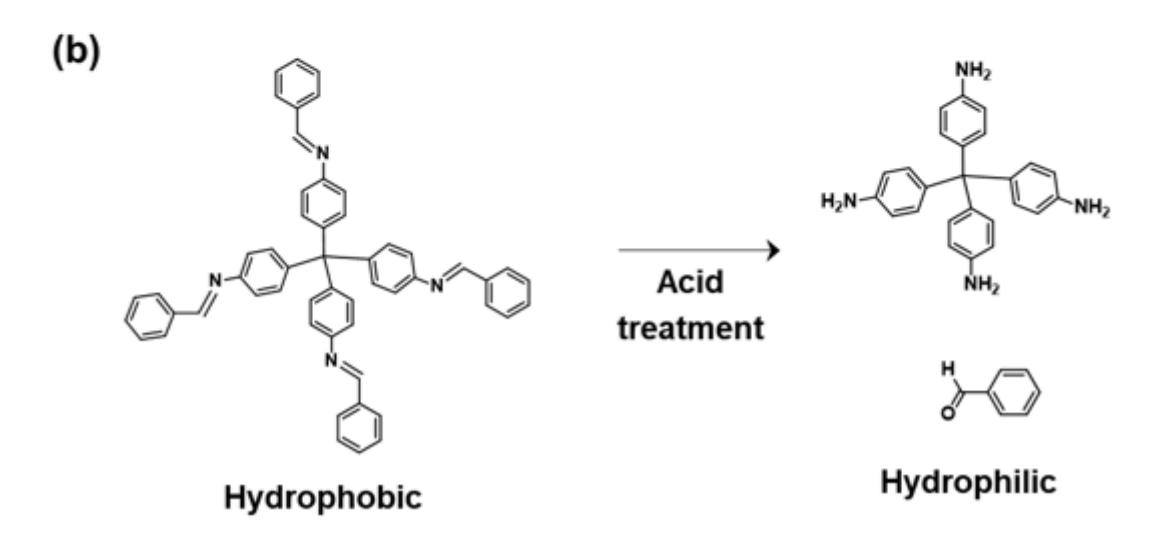


Figure 1. (a) Molecular design of acid-sensitive molecular glasses featuring a bulky aromatic core to prevent crystallization and acid-labile imine bonds. (b) Chemical structure of representative Imine₄ (*left*) and degradation products (*right*) formed under acidic conditions.

Results and Discussion

Design of Acid-Sensitive Molecular Glasses

The initial design of our acid-sensitive molecular glasses consisted of three features: a bulky aromatic core to inhibit crystallization, peripheral phenyl groups that render the starting molecular glass hydrophobic, and acid-sensitive functionality that causes a switch from

hydrophobic to hydrophilic upon deprotection. This change in hydrophilicity is key for good performance as a removable protective layer because the hydrophobic nature of the as-cast molecular glass minimizes water uptake after application but it becomes soluble when exposed to dilute aqueous acid (vide infra). Preliminary experiments screened a variety of different acidsensitive functionality starting from either hydrophilic (1) tris(4-hydroxyphenyl)ethane through functionalization with methyl or tert-butoxycarbonyl (Boc) (Figures S1–S2) or (2) tris(4-aminophenyl)methane through functionalization of the primary amines with nBoc, maleimide, or imines (Figures S3–S6). Synthetic details and characterization of the various derivatives are provided in Figures S1-S6. The acid sensitivity of these different molecular glasses was tested using solutions of sulfuric acid that are common in the semiconductor industry. First, each molecular glass was deposited on a silicon (Si) wafer by spin coating 30 μL of a 4 wt% solution in THF at 2k RPM for 30 s. The spin coated films were then dipped in solutions of H₂SO₄ (aq) (0–71 v/v%) for 3 seconds and rinsed in deionized water. The results of these acid-sensitivity tests are summarized in Table 1. While most of the acid-labile groups required H₂SO₄ (aq) concentrations as high as 71 v/v% in order to induce sufficient imine hydrolysis to become soluble, the imine-functionalized derivative required only 6 v/v%. The mechanism of imine hydrolysis involves attack of protonated iminium by water to cleave an imine bond into one amine and aldehyde. Hydrolysis is accelerated under acidic conditions, which likely explains the high acid sensitivity observed here.⁴¹

Table 1. Summary of acid-sensitivity tests for protected molecular glasses with various acidlabile groups using aqueous solutions of H₂SO₄.

Aromatic core	Acid-labile group				
\(\bar{\pi}\)	- }- o	+.L.L	**************************************	₽	-{-N ₀ CH-√_
XO*OX	Methyl R = C-CH ₃	Boc R = C-CH ₃	nBoc R = CH	Maleimide R = CH	Imine R = CH
Concentration of H ₂ SO ₄ (aq) ^a	71 v/v%	71 v/v%	71 v/v%	71 v/v%	6 v/v%

^aMinimum acid concentration for removal in 3 seconds.

To better understand the products after deprotection, we tracked the extent of reaction over time with ¹H nuclear magnetic resonance spectroscopy (NMR) using representative solutions containing 0.05 moles of the imine- or nBoc-derived molecular glasses and 1 mole of H₂SO₄ in 8:92 vol% D₂O:DMSO-*d*₆. Immediately after preparation, the NMR spectrum of each mixture was collected to represent the initial state (Figures 2a and 2c). For Imine molecules, a sharp peak at 9.8 ppm originating from the formation of aldehyde was observed within a few seconds (Figure 2b). Simultaneously, the characteristic imine resonance at 9.3 ppm disappeared. These observations are consistent with hydrolysis of the imine into an aldehyde and primary amine. In contrast, a clear amide peak at 9.1 ppm remained for the nBoc glass even after adding 1 mole H₂SO₄ (Figure 2d). From these results, imine functionality clearly provides the fastest deprotection kinetics and was selected for further studies.

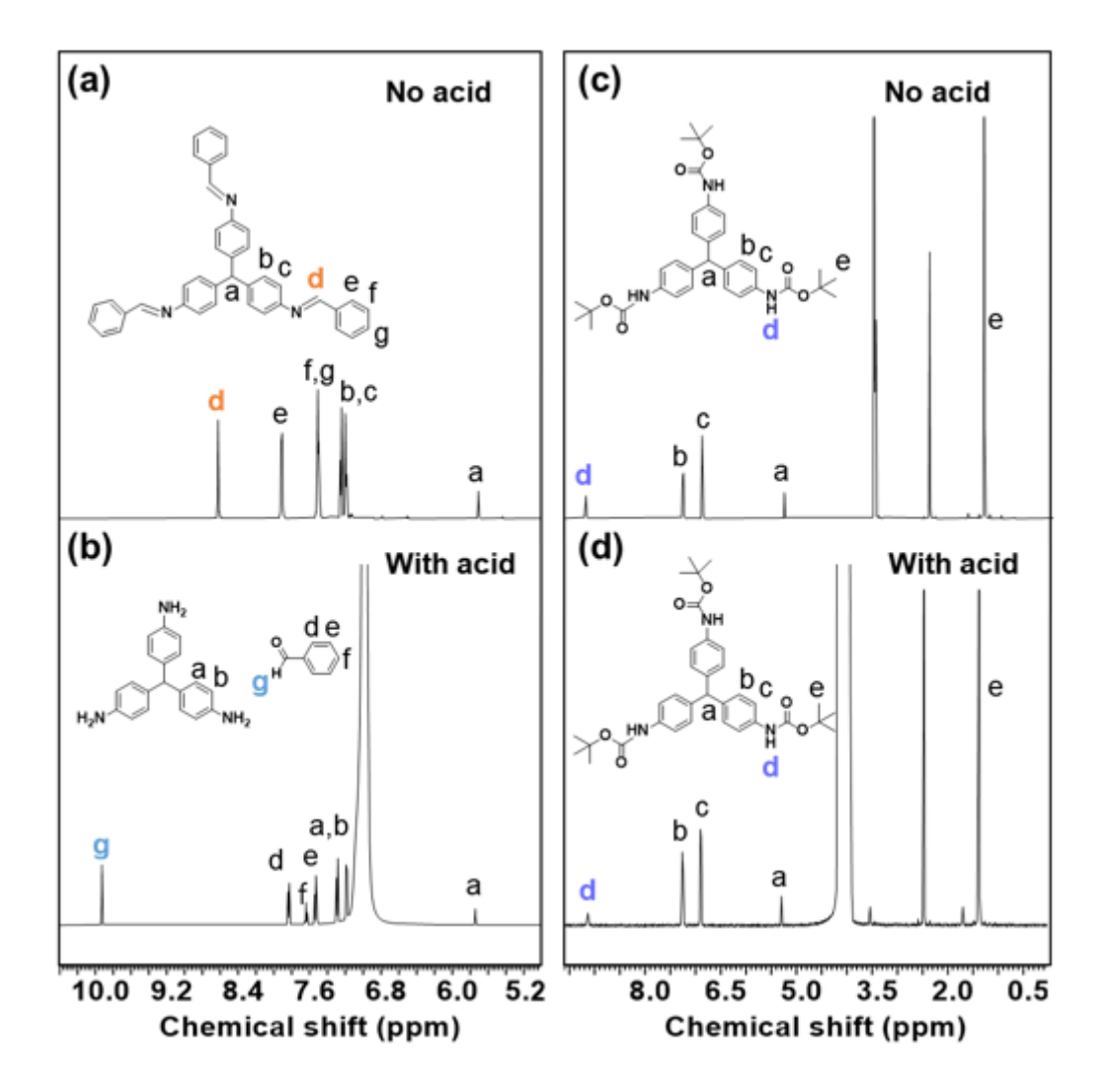


Figure 2. Hydrolysis of (a, b) imine bonds surrounding a molecular glass core is significantly faster than (c,d) a *tert*-butoxycarbonyl derivative as measured by 1 H NMR. For both experiments, spectra were collected before and after added 1 mole of aqueous sulfuric acid to a solution of the molecular glass (0.05 moles) in a solution of 8:92 v/v% $D_2O:DMSO-d_6$.

The ability to tune acid sensitivity of imine-protected molecular glasses was further examined by varying the number of imine groups per molecule (n). We complemented the n = 3 derivative described above (denoted Imine₃) by synthesizing analogues with two or four imine groups per molecule by functionalization of bis(4-aminophenyl)methane and tetrakis(4-aminophenyl)methane, respectively. The synthetic procedures used to synthesize Imine₂ and

Imine₄ are described in Figures S7-S12. Like Imine₃, Imine₂ and Imine₄ undergo acidcatalyzed hydrolysis as evidenced by ¹H NMR experiments (Figures S13–14). To further study the relative degradation kinetics of imine-functionalized molecular glasses, UV-vis absorbance was monitored as a function of time (Figure 3 and Figures S15–S17). 44 At t = 0 minutes, the maximum absorbance at 330 nm ($A_{330 \text{ nm}}$) for all three derivatives originates from the $n-\pi^*$ transition associated with the imine group (just Imine₄ is shown in Figure 3a for clarity).⁴⁵ Upon adding $10 \,\mu\text{L}$ of $6 \,\text{v/v}\%$ H₂SO₄ (aq), the intensity of $A_{330\text{nm}}$ rapidly decreases. The kinetics of this reaction were analyzed by normalizing $A_{330\text{nm}}$ with its initial value at t = 0 (Figure 3b). The slope of these plots suggests pseudo first-order kinetics as expected for acid-catalyzed hydrolysis. 46,47 Imine₄ undergoes faster hydrolysis than Imine₃ and Imine₂ as evidenced by the extracted rates: 0.48 s⁻¹, 0.29 s⁻¹, 0.24 s⁻¹, respectively (Figures S15-S17). As a control, hydrolysis in the absence of any acid was also investigated using ¹H NMR (Figure S18). Under these conditions, hydrolysis was observed in the Imine₄ solution only after 2 days. Acid therefore greatly accelerates imine hydrolysis. An inverse relationship between the kinetic rate of degradation and the number of imine groups per molecule confirms that the acid-sensitivity of these protected molecular glasses is readily tuned by adjusting the number of imine groups per molecule.

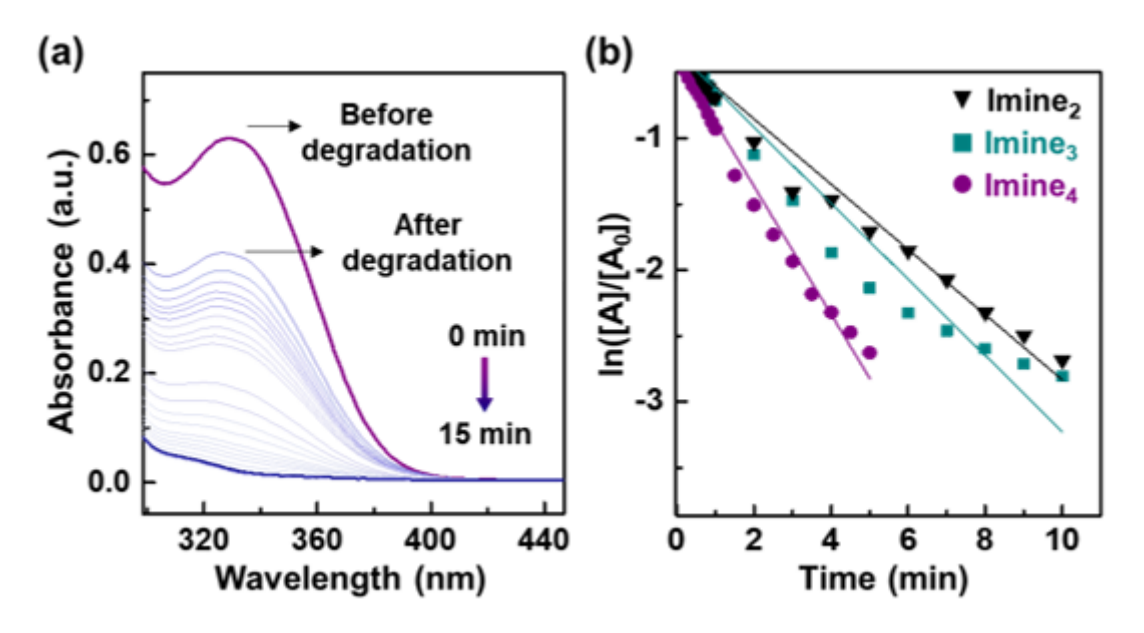


Figure 3. (a) UV–vis absorption can be used to monitor the deprotection kinetics of imine-based molecular glasses in a solution of dimethyl sulfoxide and aqueous H₂SO₄. The trend observed in the absorption spectra of Imine₄ (as shown) is also representative of Imine₂ and Imine₃. (b) More imine groups per molecular result in faster hydrolysis. There is also an inverse relationship between the number of imine groups per molecule and the concentration of H₂SO₄ required to induce degradation as summarized in Table S1. Collectively, these results indicate the acid sensitivity of molecular glasses can be readily tuned by adjusting the number of imine groups per molecule.

Uniform Films with Hydrophilicity Switching

After identifying imine-based molecular glasses as a promising platform for acidcatalyzed deprotection, their performance in thin films was studied. First, Imine₂, Imine₃ and Imine₄ were spin-coated from 4 wt% solutions in THF at 2k rpm for 30 s onto silicon substrates with native oxide, yielding smooth films with a thickness circa 68 nm as measured by ellipsometry (Figure S19). All three films can be cleanly removed in a short period of time by dipping in dilute sulfuric acid as observed visually. Again, the necessary dip time correlates with the number of imine groups per molecular: in 1 v/v% of H₂SO₄ (aq), Imine₄ was removed in 30 sec, while Imine₃ required 2 min and Imine₂ 4 min. Representative images for Imine₄ before and after removal are shown in Figures 4a (see also Figure S20). These results highlight the facile removal of imine-protected molecular glasses in dilute H₂SO₄ (aq). Because acidic solutions are used in many semiconductor unit processes (*e.g.* electroplating and wafer cleaning), these acid-sensitive protective coatings can be used directly without needing a separate removal step.

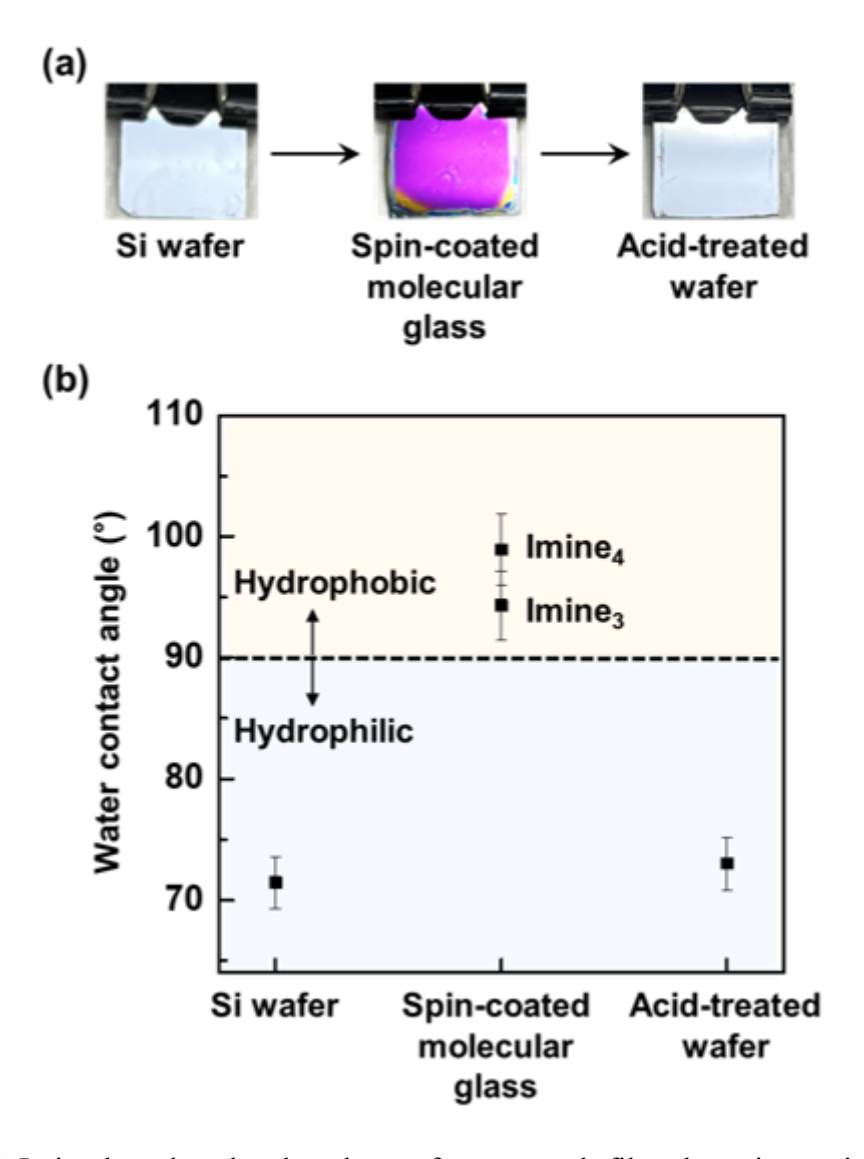


Figure 4. (a) Imine-based molecular glasses form smooth films by spin coating that can be cleanly removed in aqueous sulfuric acid. (b) Water contact angles are consistent with a

hydrophobic-hydrophilic switch after acid treatment. Error bars represent the average and standard deviation of three repeated measurements.

In order to confirm the complete removal of acid-sensitive molecular glasses and the ability to recover a pristine surface, we measured water contact angles 48,49 (θ) of samples before and after acid treatment (Figure 4b). Deionized water contact angles were measured at the liquid–solid interface, where the solid was either an initial Si wafer, protective coating, or (bare) Si wafer after acid treatment. For the initial Si wafer containing a native oxide layer, $\theta_{\text{Si,initial}} = 71^{\circ}$ is indicative of a moderately hydrophilic surface. Once the Si wafer was coated with either Imine₃ or Imine₄, a significant increase in $\theta_{\text{Imine}3} = 98^{\circ}$ and $\theta_{\text{Imine}4} = 100^{\circ}$ is evidence that the coatings are more hydrophobic. This result is not surprising since Imine₃ and Imine₄ contain hydrophobic aromatic groups. With subsequent acid treatment, the protective coatings were removed, recovering the initial state $\theta_{\text{Si,recovered}} = 75^{\circ}$ of the native oxide within measurement error. Imine₃ and Imine₄ layers are therefore completely removed upon exposure to a solution of acid.

Having established the exquisite acid-sensitivity of Imine₄—a result of having four imine bonds per molecule—we analyzed its thin films with a variety of techniques to assess their uniformity and structure (Figure 5a). After solvent evaporation, the surface was flat and uniform by atomic force microscopy (AFM, Figure 5b). From the AFM data, an estimate of the root-mean-square roughness (R_q) was extracted (Figure 5d) along the white line shown in Figure 5b. The resulting $R_q = 0.4$ nm indicates these spin coated films are highly uniform. In theory, the long-term stability of molecular glasses should enhance the utility of protective thin films because they are not prone to crystallization⁵⁰ that can cause feature collapse on patterned wafers. We assessed the thin-film structure of Imine₄ with grazing-incidence wide-angle X-ray

scattering (GIWAXS) to confirm that it is indeed amorphous. As shown in Figure 5c, a two-dimension GIWAXS pattern of Imine₄ contains no peaks or rings in the q range 0.2 Å⁻¹ to 2 Å⁻¹ that would indicate long-range order. A slight halo at q = 1.3 Å⁻¹ is present, but this feature is common in glassy materials with a typical intermolecular distance of about 4.8 Å. Figure 5e shows an azimuthal scan at q = 1.3 Å—the lack of peaks is further confirmation that the material is amorphous.⁵¹ Similar results were obtained for Imine₃ (Figure S21). This behavior for both Imine₃ and Imine₄ is consistent with the bulk, where only one T_g and no crystallization or melting is observed by differential scanning calorimetry (Figure S22). Clearly, this material design featuring a non-planar bulky core minimizes close packing that would cause crystallization. Notably, spin-coated Imine₄ films were stable indefinitely without any obvious shrinkage or change in color (*i.e.* from sluggish crystallization) under ambient conditions for over at least 5 months.

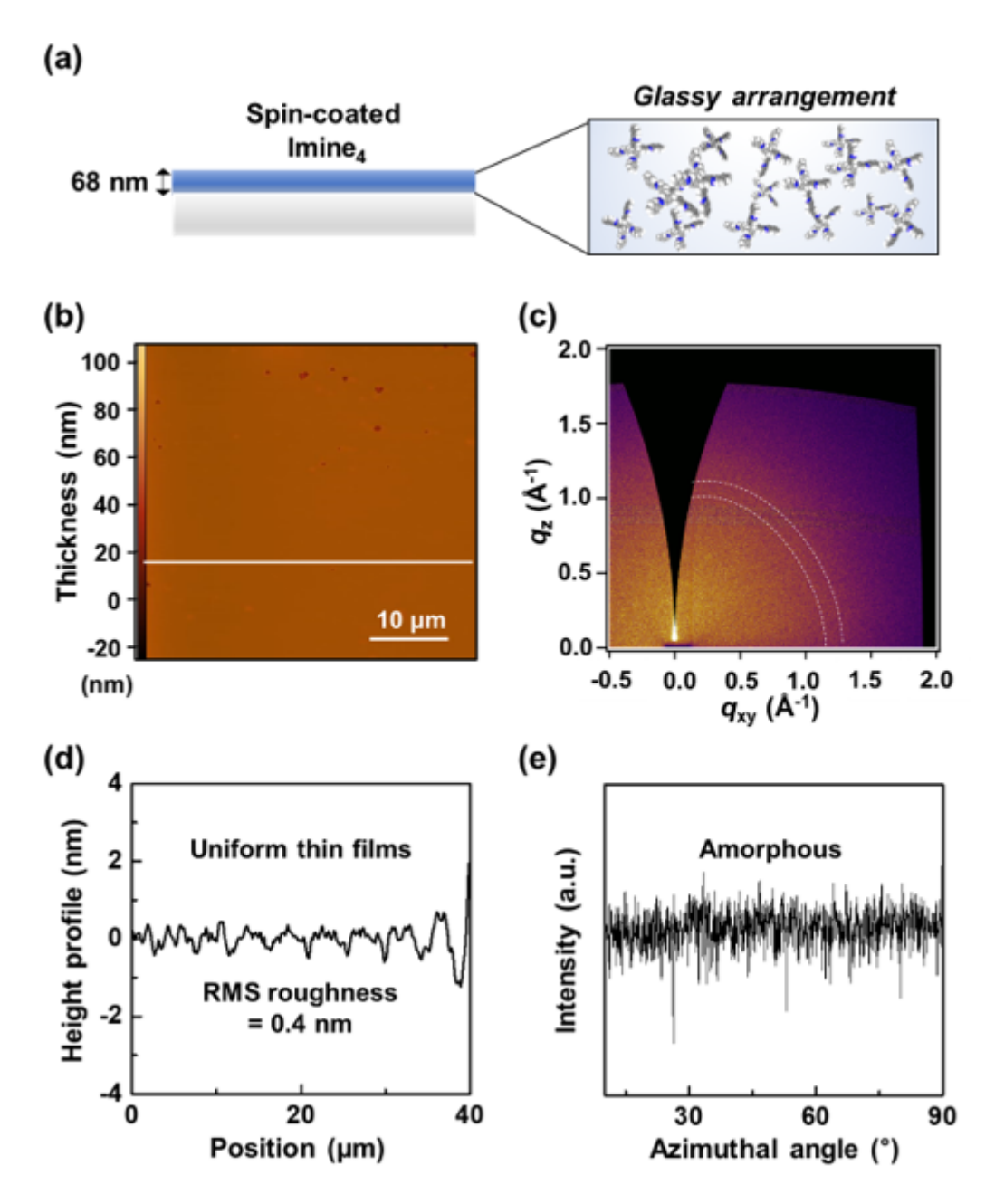


Figure 5. (a) Thin films of Imine₄ are uniform, flat, and amorphous as evidenced by (b,d) atomic force microscopy and (c,e) grazing-incidence X-ray scattering. In (e), the azimuthal profile is shown at $q = 1.3 \text{ Å}^{-1}$.

Efficient Protection Against Oxidation

Next, to study the efficacy of Imine4 thin films at preventing Cu oxidation, a series of experiments was designed that leverage X-ray photoelectron spectroscopy (XPS, Figure 6a). First, a Cu wafer was loaded into the spectrometer and native oxide was removed by sputtering with a monatomic ion beam for 20 s under vacuum. The surface of the wafer was scanned before and after sputtering, with the amount of oxygen reduced from 65.7% (Figure S23) to 1%. Next, the etched Cu wafer was loaded into an air-free sample holder to minimize air exposure while transferring it from the XPS chamber to a spin coater. Once there, a solution of 4 wt% Imine₄ in THF was immediately spin coated onto the etched wafer. Note that spin coating was performed under ambient conditions, so brief exposure to oxygen during this step was unavoidable. The coated wafer was then stored under ambient conditions for different amounts of "queue" time up to 120 h. After placing the sample back into the XPS, depth profiling with an argon cluster gun was used to directly measure the Imine₄-Cu interface and quantify any oxide regrowth underneath the protective coating. 52,53 This set of steps constitutes the bottom path shown in Figure 6a. Additional control experiments were performed on etched Cu wafers that were not coated with Imine₄, on which significant oxide regrowth is expected during storage under ambient conditions as a baseline for comparison (the top path in Figure 6a).

The oxidation of Imine₄-coated Cu wafers was first monitored on shorter time scales between 1–6 h. As an example, Figure S24 shows the depth profile through an Imine₄-protected Cu wafer that had been exposed to air for 2 hours. At short etch times, the only detected signals come from the N1s at 398.1 eV and C1s at 284.8 eV, which is consistent with the elements that make up Imine₄. As the etch time increases, Cu(2p_{1/2}), Cu(2p_{3/2}) (958–925 eV), and O1s (530 eV) peaks appear while the intensity of the N1s and C1s peaks decreases. This indicates that the Imine₄ protective coating is being removed and the molecular-glass–wafer interface probed

underneath. With sufficient etching, the N1s (and C1s) peaks are greatly suppressed, suggesting the Imine₄ coating has been completely removed. Quantitatively, the relative atomic percentages of nitrogen, copper, and oxygen were calculated at each etching interval from their respective high-resolution scans (Figure S25). These calculated values were plotted against etching time to highlight the change in each element throughout the depth profile (Figure S26). For the depth profile following a 2 h exposure to air, nitrogen drops from 100% to 0% over 800 sec of etching. Simultaneously, copper and oxygen increase from 0% to 83% and 0% to 17%, respectively. Results for air exposure times of 1, 2, 4, and 6 hours are also available in the Figures S25–S26. Notably, for Imine₄-protected samples, the percent oxygen measured underneath the molecular glass for each queue time did not change appreciably between 1–6 hours, consistently staying at approximately 17% (Figure S26).

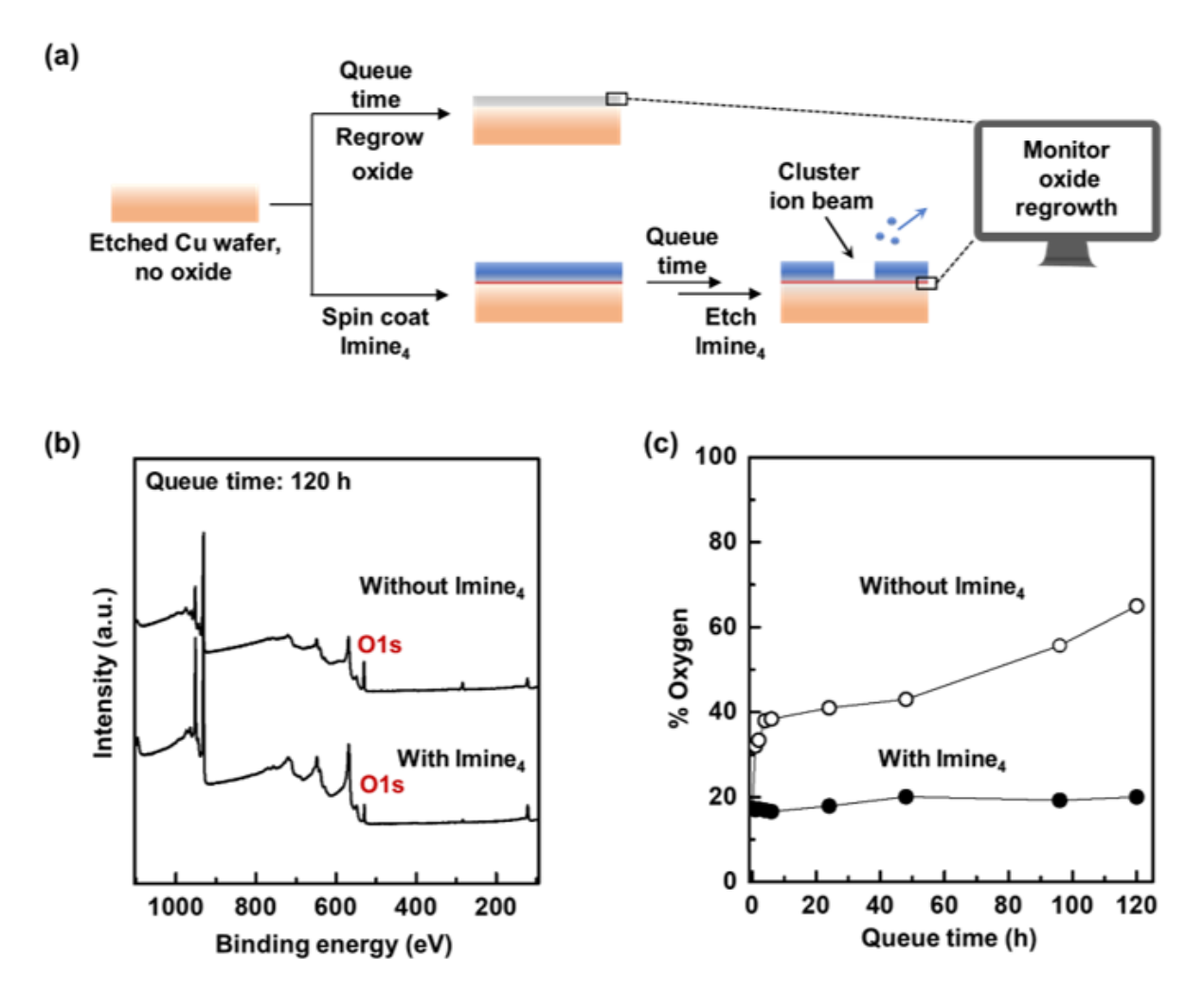


Figure 6. (a) Design of an XPS-based experiment to measure the surface protection afforded by molecular glasses. (b) XPS survey scans of an etched Cu wafer with and without a protective Imine₄ layer after 120 h of queue time. The stronger O1s peak is evident in the control sample without Imine₄. (c) Quantitative analysis of the atomic % oxygen extracted from either XPS survey scans [like shown in (b)] or high-resolution scans indicates oxide regrowth underneath an Imine₄ thin film is significantly reduced compared to a bare Cu wafer, even after extended queue times.

Oxidation underneath Imine₄-coated wafers was also monitored over longer periods of air exposure up to 120 h. Survey and high-resolution XPS depth profile scans of Imine₄-coated

Cu wafers are presented in Figures S27–S28. As a control, the oxidation of Cu wafers that were etched, but not coated, was also tracked (Figure S29). Figure 6b shows survey XPS depth profiles of an etched Cu wafer with and without Imine₄ after 120 h. The intensity of the O1s (530 eV) peak is significantly higher than for the Cu control. The level of Cu oxidation for coated samples compared to non-coated controls over the course of 120 h is summarized in Figure 6c. In all cases, the molecular glass significantly reduces wafer oxidation; the percentage of oxygen measured at the molecular-glass—wafer interface was always less than 20%, even after 120 h of exposure to air, compared to >60% with bare Cu. We suspect some, if not all, of this initial oxidation underneath the molecular glass is a result of the brief exposure to air during spin coating (Figures S30–S33), which could be prevented if the spin coater was placed in an inert atmosphere. These results highlight the efficiency of Imine₄ coatings as protective layers that reduce the oxidation of underlying materials such as Cu. Finally, the utility of molecular glasses in preventing surface oxidation may extend readily to other surfaces of interest as they form reasonably uniform thin films on silicon, cobalt, titanium nitride, and even patterned substrates with aluminum oxide lines on native silicon oxide in Figure S34.

Conclusions

Acid-sensitive molecular glasses are efficient protective coatings that can be easily applied by spin coating and removed in dilute solutions of aqueous acid. Key molecular-design features include: (i) a bulky core to inhibit crystallization, (ii) acid-sensitive imine groups, and (iii) an aromatic periphery; the latter two facilitate a hydrophobic-to-hydrophilic switch upon hydrolysis in sulfuric acid solutions as low as 1 vol%. Kinetic studies revealed that acid-sensitivity is significantly increased with a larger number of protecting groups per molecule. Solution-processed thin films of these molecular glasses are easy to apply, uniform, and

amorphous. Quantitative analysis by X-ray photoelectron spectroscopy indicates molecular glasses prevent oxidation of a pristine copper surface for at least 120 h with a greater-than threefold decrease in oxidation relative to uncoated control samples. These results establish the potential of molecular glasses to serve as easily removable protective coatings that are compatible with contemporary semiconductor processes.

Experimental

Synthesis

Imine₄: Tetrakis(4-aminophenyl)methane (0.44 mmol, 0.17 g) was dissolved in EtOH/DMF (v/v =1:1). Benzaldehyde (1.97 mmol, 0.209 g) was added dropwise into the solution, and the mixture was refluxed at 70 °C for 48 h. A yellowish solid was filtered and rinsed with methanol and ethanol. The crude product was purified by recrystallization in hot THF. The product was obtained as an ivory powder (yield: 58%). ¹H NMR (600 MHz, DMSO- d_6): δ = 7.25 (s, ArH, 16H), 7.48 – 7.52 (d, ArH, 12H), 7.89 – 7.92 (d, ArH, 8H), 8.64 (s, NCH, 4H). ¹³C NMR (125 MHz, DMSO- d_6): δ = 63.8 120.95, 129.11, 129.27, 131.67, 136.48, 144.71, 149.70, 161.28. MALDI-ToF (ESI⁺) Exact mass calc for C₅₃H₄₀N₄ [M]: 732.3253, found [M+H]⁺: 733.460. Imine₂ and Imine₃ were synthesized using above synthetic procedure described in Supporting Information.

General methods

Materials preparation: Proton (1 H) and carbon (13 C) nuclear magnetic resonance (NMR) spectra were collected on a 600 MHz SB Varian VNMRS. The chemical shifts were measured in parts per million (ppm) downfield. Samples were prepared in deuterated dimethyl sulfoxide (DMSO- d_6). 1 H and 13 C NMR spectra were referenced using the residual solvent signal as the internal standard (DMSO- d_6 , 1 H 2.5 ppm, 13 C 39.52 ppm). FT IR was measured

with a Thermo Nicolet iS10 FTIR Spectrometer equipped with a Smart Diamond attenuated total reflectance (ATR) accessory. The resolution of FT IR was 1 cm⁻¹ and 40 scans were averaged for the spectra. The molecular weight of Imine₄ molecules was determined using a Bruker (Bruker Daltonics, Billerica, MA) Microflex LRF MALDI TOF mass spectrometer. Electrospray ionization (ESI) source were positive ions.

Surface characterization on spin-coated molecular glasses. Contact angle (θ) was measured by contact angle analyzer (Model 200 Standard Contact Angle Goniometer with DROPimage Standard) by introducing 5 μ l water droplets of molecular glasses spin coated onto the silicon wafers. UV-visible absorption spectra were collected by Agilent Technologies, Cary 60 spectrophotometer using a rectangular quartz cell with a 10.0 mm path length.

Molecular glass behavior. Thermal transition behavior was studied using differential scanning calorimetry (DSC, Perkin-Elmer). For DSC experiments, sample weights were controlled to be about 3.5 mg and the pan weights were kept constant with a precision of ± 0.001 mg. Topographic images were collected with an atomic force microscope (AFM, Asylum MFP-3D standard system w/low force indenter). Thickness of spin-coated films were measured with a J.A. Wollam Co. alpha-SE ellipsomer. Grazing Incident Wide Angle X-ray Scattering (GIWAXS) experiments were performed using a diffractometer with an X-ray source XENOCS Genix 50W x-ray micro source with a monochromator XENOCS FOX2D multilayer optics with a detector Dectris EIGER 1M, 77.2 mm x 79.9 mm sensitive area 1030 x 1065 32-bit image.

Etching native oxide on copper wafer and protection tests. X-ray photoelectron spectroscopy (XPS) was conducted using a ThermoFisher Escalab Xi+ using Al Kα X-ray radiation in combination with an electron flood gun. To etch the native oxide layer on bare copper-coated wafer, a monatomic ion beam (Ar+ ions) with 2 keV energy was used to etch an

area (1.25 ×1.25 mm²) of the wafer. For depth profiling, an argon cluster ion beam (2 keV energy, 1,000 cluster size) was used to etch the Imine₄ layer that had been spin coated onto the etched copper-coated wafer. The etched area was 1.25 ×1.25 mm² in size. All spectra were referenced to the C 1s peak (284.8 eV).

ASSOCIATED CONTENT

Supporting Information

The Supporting Information is available free of charge on the ACS Publications website: Materials, ¹H and ¹³C NMR, MALDI-ToF spectra, Tables of acid-sensitivity test, FT IR spectrum, UV-Vis spectra, Ellipsometry data, GIWAXS pattern and corresponding 1D pattern, DSC thermograms, XPS survey scan/high-resolution scan spectra, and Atomic %

AUTHOR INFORMATION

Corresponding Author

Christopher M. Bates* (E-mail: cbates@ucsb.edu).

Author Contributions

The manuscript was written through the contributions of all authors. ACKNOWLEDGMENT

This work was partially supported by Lam Research Corporation (synthesis) and the National Science Foundation under Award No. CMMI-2053760 (characterization). C.M.B. thanks The Camille and Henry Dreyfus Foundation for partial support. We gratefully acknowledge use of the laboratory for surface characterization within the California NanoSystems Institute, supported by the University of California, Santa Barbara and the University of California, Office of the President. The research reported here made use of shared

facilities of the UCSB MRSEC (NSF DMR-2308708), a member of the Materials Research Facilities Network (www.mrfn.org).

REFERENCES

- (1) Zhou, F.; Li, Z.; Shenoy, G. J.; Li, L.; Liu, H. Enhanced Room-Temperature Corrosion of Copper in the Presence of Graphene. *ACS nano* **2013**, *7*, 6939–6947.
- (2) Luo, X.; Zhong, J.; Zhou, Q.; Du, S.; Yuan, S.; Liu, Y. Cationic Reduced Graphene Oxide as Self-Aligned Nanofiller in the Epoxy Nanocomposite Coating with Excellent Anticorrosive Performance and its High Antibacterial Activity. *ACS Appl. Mater. & interfaces* **2018**, *10*, 18400–18415.
- (3) Shabnam, P.; Sharif, A. Synergistic Effects of Linseed Oil Based Waterborne Alkyd and 3-Isocynatopropyl Triethoxysilane: Highly Transparent, Mechanically Robust, Thermally Stable, Hydrophobic, Anticorrosive Coatings. *ACS Sustain. Chem. Eng.* **2016**, *4*, 3062–3075.
- (4) Renner, F. U.; Stierle, A.; Dosch, H.; Kolb, D. M.; Lee, T.-L.; Zegenhagen, J. Initial Corrosion Observed on the Atomic Scale. *Nature* **2006**, *439*, 707–710.
- (5) Lee, U.; Han, Y.; Lee, S.; Kim, J. S.; Lee, Y. H.; Kim, U. J.; Son, H. Time Evolution Studies on Strain and Doping of Graphene Grown on a Copper Substrate using Raman Spectroscopy. *ACS Nano* **2019**, *14*, 919–926.
- (6) Wang, K.; Le, J. B.; Zhang, S. J.; Ren, W. F.; Yuan, J. M.; Su, T. T.; Chi, B. Y.; Shao, C. Y.; Sun, R. C. A Renewable Biomass-Based Lignin Film as an Effective Protective Layer to Stabilize Zinc Metal Anodes for High-Performance Zinc–Iodine Batteries. *J. Mater. Chem. A* 2022, 10, 4845–4857.
- (7) Li, S.; Huang, J., Cui, Y.; Liu, S.; Chen, Z.; Huang, W.; Li, C.; Liu, R.; Fu, R.; Wu, D. A Robust All-Organic Protective Layer Towards Ultrahigh-Rate and Large-Capacity Li Metal Anodes. *Nat. Nanotech.* **2022**, *17*, 613–621.
- (8) Han, Z.; Zhang, C.; Lin, Q.; Zhang, Y.; Deng, Y.; Han, J.; Wu, D.; Kang, F.; Yang, Q. H.; Lv, W. A Protective Layer for Lithium Metal Anode: Why and How. *Small methods* **2021**, *5*, No. 2001035.
- (9) Li, J.; Li, Y.; Wang, Z.; Bian, H.; Hou, Y.; Wang, F.; Xu, G.; Liu, B.; Liu, Y. Ultrahigh Oxidation Resistance and High Electrical Conductivity in Copper-Silver Powder. *Sci. Rep.* **2016**, *6*, No. 39650.
- (10) Yang, C.; Cai, H.; Cui, S.; Huang, J.; Zhu, J.; Wu, Z.; Ma, Z.; Fu, R. K.; Sheng, L.; Tian, X.; Chu, P. K. A Zinc-Doped Coating Prepared on the Magnesium Alloy by Plasma Electrolytic Oxidation for Corrosion Protection. *Surf. Coat. Technol.* **2022**, *433*, No. 128148.
- (11) Redondo, M. I.; Breslin, C. B., Polypyrrole Electrodeposited on Copper from an Aqueous Phosphate Solution: Corrosion Protection Properties. *Corros. Sci.* **2007**, *49*, 1765–1776.

- (12) Toorani, M.; Aliofkhazraei, M.; Mahdavian, M.; Naderi, R., Effective PEO/Silane Pretreatment of Epoxy Coating Applied on AZ31B Mg Alloy for Corrosion Protection. *Corros. Sci.* **2020**, *169*, No. 108608.
- (13) Kosec, T.; Milošev, I.; Pihlar, B. Benzotriazole as an Inhibitor of Brass Corrosion in Chloride Solution. *Appl. Sur. Sci.* **2007**, *253*, 8863–8873.
- (14) Gnedenkov, S. V.; Sinebryukhov, S. L.; Mashtalyar, D. V.; Egorkin, V. S.; Sidorova, M. V.; Gnedenkov, A. S. Composite Polymer-Containing Protective Coatings on Magnesium Alloy MA8. *Corros. Sci.* 2014, 85, 52–59.
- (15) Kim, Y. J.; Lee, H.; Noh, H.; Lee, J.; Kim, S.; Ryou, M. H.; Lee, Y. M.; Kim, H. T. Enhancing the Cycling Stability of Sodium Metal Electrodes by Building an Inorganic—Organic Composite Protective Layer. *ACS Appl. Meter. & interfaces* **2017**, *9*, 6000–6006.
- (16) Norrman, K.; Ghanbari-Siahkali A.; Larsen N. B. Studies of Spin-Coated Polymer Films. *Annu. Rep. Prog. Chem., Sect. C*, **2005**, *101*, 174–201.
- (17) Li, W.; Sun, Q.; Li, L.; Jiu, J.; Liu, X.-Y.; Kanehara, M.; Minari, T.; Suganuma, K. The Rise of Conductive Copper Inks: Challenges and Perspectives. *Appl. Mater. Today*, **2020**, *18*, No. 100451.
- (18) Farahati, R.; Ghaffarinejad, A.; Mousavi-Khoshdel, S. M.; Rezania, J.; Behzadi, H.; Shockravi, A. Synthesis and Potential Applications Some Thiazoles as Corrosion Inhibitor of Copper in 1 M HCl: Experimental and Theoretical Studies. *Prog. Org. Coat.* **2019**, *132*, 417–428.
- (19) Laibinis, P. E.; Whitesides, G. M. Self-Assembled Monolayers of *n*-Alkanethiolates on Copper are Barrier Films that Protect the Metal Against Oxidation by Air. *J. Am. Chem. Soc.*, **1992**, *114*, 9022–9028.
- (20) Jennings, G. K.; Laibinis, P. E. Self-Assembled Monolayers of Alkanethiols on Copper Provides Corrosion Resistance in Aqueous Environments. *Colloids Surf. A: Physicochem. Eng.* **1996**, *116*, 105–114.
- (21) Li, J.; Mayer, J. W.; Colgan E. G. Oxidation and Protection in Copper and Copper Alloy Thin Film. *J. Appl. Phys.* **1991**, *70*, 2820–2827.
- (22) Kovačević, N.; Milošev, I.; Kokalj, A. The Roles of Mercapto, Benzene, and Methyl Groups in the Corrosion Inhibition of Imidazoles on Copper: II. Inhibitor–Copper Bonding. *Corros. Sci.* **2015**, *98*, 457–470.
- (23) Brusic, V.; Frisch, M. A.; Eldridge, B. N.; Novak, F. P.; Kaufman, F. B.; Rush, B. M.; Frankel, G. S. Copper Corrosion with and without Inhibitors. *J. Electrochem. Soc.* **1991**, *138*, 2253–2259.
- (24) Finšgar, M.; Milošev, I. Inhibition of Copper Corrosion by 1,2,3-Benzotriazole: A Review. *Corros. Sci.* **2010**, *52*, 2737–2749.
- (25) Chen, S.; Brown, L.; Levendorf, M.; Cai, W.; Ju, S. Y.; Edgeworth, J.; Li, X.; Magnuson, C. W.; Velamakanni, A.; Piner, R. D.; Kang, J. Oxidation Resistance of Graphene-Coated Cu and Cu/Ni Alloy. *ACS Nano* **2011**, *5*, 1321–1327.
- (26) Ediger, M. D.; Harrowell, P. Perspective: Supercooled Liquids and Glasses. *Chem. Phys.* **2012**, *137*, No. 080901.

- (27) Shirota, Y.; Kageyaman, H. 1-Small Molecular Weight Materials for (Opto)Electronic Applications: Overview. *In Handbook of Organic Materials for Optical and (Opto) Electronic Devies: Properties and Applications*: Woodhead Publish, **2013**; pp. 3–82.
- (28) Silva, A. D.; Sundberg, L. K.; Ito, H.; Sooriyakumaran, R.; Allen, R. D.; Ober, C. K. A Fundamental Study on Dissolution Behavior of High-Resolution Molecular Glass Photoresists. *Chem. Mater.* **2008**, *20*, 7292–7300.
- (29) Cragnolion, G. A. 2-Corrosion Fundamentals and Characterization Techniques. In *Techniques for corrosion monitoring*, Woodhead Publishing **2022**; pp. 7–42.
- (30) Hancock, B. C.; Zografi, G. Characteristics and Significance of the Amorphous State in Pharmaceutical Systems, *J. Pharm. Sci.* **1997**, *86*, 1–12.
- (31) Chan, L. H.; Lee, R. H.; Hsieh, C. F.; Yeh, H. C.; Chen, C. T. Optimization of High-Performance Blue Organic Light-Emitting Diodes Containing Tetraphenylsilane Molecular Glass Materials. *J. Am. Chem. Soc.* **2002**, *124*, 6469–6479.
- (32) Strohriegl, P.; Grazulevicius, J. V. Charge-Transporting Molecular Glasses. *Adv. Mater.* **2002**, *14*, 1439–1452.
- (33) De Silva, A.; Felix, N. M.; Ober, C. K. Molecular Glass Resists as High-Resolution Pattering Materials, *Adv. Mater.* **2008**, *20*, 3355–3361.
- (34) Yang, D.; Chang, S. W.; Ober, C. K. Molecular Glass Photoresists for Advanced Lithography, *J. Mater. Chem.* **2006**, *16*, 1693–1696.
- (35) Davis, V. K.; Bates, C. M.; Omichi, K.; Savoie, B. M.; Momčilović, N.; Xu, Q.; Wolf, W. J.; Webb, M. A.; Billings, K. J.; Chou, N. H.; Alayoglu, S.; Mckenney, R. K.; Darolles, I. M.; Nair, N. G.; Hightower, A.; Rosenberg, D.; Ahmed, M.; Brooks, C. J.; Miller III, T. F.; Grubbs, R. H.; Jones, S. C. Room-Temperature Cycling of Metal Fluoride Electrodes: Liquid Electrolytes for High-Energy Fluoride Ion Cells. *Science*, 2018, 362, 1144–1148.
- (36) Lebel, O.; Soldera, A. 9 Molecular Glasses: Emerging Materials for the Next Generation. *Adv. Mater.* **2020**, 239, edited by Lebel, O.; Soldera, A.
- (37) De Silva, A.; Lee, J. K.; André, X.; Felix, N. M.; Cao, H. B.; Deng, H.; Ober, C. K. Study of the Structure–Properties Relationship of Phenolic Molecular Glass Resists for Next Generation Photolithography. *Chem. Mater.* **2008**, *20*, 1606–1613.
- (38) Lawson, R. A.; Lee, C. T.; Henderson, C. L.; Whetsell, R.; Tolbert, L.; Yueh, W.; Influence of Solubility Switching Mechanism on Resist Performance in Molecular Glass Resists. *J. Vac. Sci. Technol.* **2007**, *25*, 2140–2144.
- (39) Swallen, S. F.; Kearns, K. L.; Mapes, M. K.; Kim, Y. S.; McMahon, R. J.; Ediger, M. D.; Wu, T.; Yu, L.; Satija, S. Organic Glasses with Exceptional Thermodynamic and Kinetic Stability. *Science*, **2007**, *315*, 353–356.
- (40) Baker, R. W. Membrane Technology and Applications. Wiley & Sons, 2004
- (41) Belowich, M. E.; Stoddart, J. F. Dynamic Imine Chemistry. *Chem. Soc. Rev.* **2012**, *41*, 2003–2024.
- (42) Chiong, J. A.; Zheng, Y.; Zhang, S.; Ma, G.; Wu, Y.; Ngaruka, G.; Lin, Y.; Gu, X.; Bao, Z. Impact of Molecular Design on Degradation Lifetimes of Degradable Imine-Based Semiconducting Polymers. *J. Am. Chem. Soc.* **2022**, *144*, 3717–3726.

- (43) Choi, C.; Self, J. L.; Okayama, Y.; Levi, A. E.; Gerst, M.; Speros, J. C.; Hawker, C. J.; Read de Alaniz, J.; Bates, C. M. Light-Mediated Synthesis and Reprocessing of Dynamic Bottlebrush Elastomers under Ambient Conditions. *J. Am. Chem. Soc.* **2021**, *143*, 9866–9871.
- (44) Kim, S.; Linker, O.; Garth, K.; Carter, K. R. Degradation Kinetics of Acid-Sensitive Hydrogels. *Polym. Degrad. Stab.* **2015**, *121*, 303–310.
- (45) Gan, W.; Zhang, Z.; Zheng, X.; Yu, Z.; Xie, C.; Wen, H.; Sun, L.; Zhao, Y. Modulation of Imine-Based Aggregation-Induced Emission Fluorescence Performance Through the Extension of Molecular Linkers. *Asian J. Org. Chem.* **2023**, *12*, No. 202200559.
- (46) Mosier, N. S.; Ladisch, C. M.; Ladisch, M. R. Characterization of Acid Catalytic Domains for Cellulose Hydrolysis and Glucose Degradation. *Biotechnol. Bioeng.* **2002**, *79*, 610–618.
- (47) Liu, B.; Thayumanavan, S. Substituent effects on the pH Sensitivity of Acetals and Ketals and Their Correlation with Encapsulation Stability in Polymeric Nanogels. *J. Am. Chem. Soc.* **2017**, *139*, 2306–2317.
- (48) Prydatko, A. V.; Belyaeva, L. A.; Jiang, L.; Lima, L. M.; Schneider, G. F. Contact Angle Measurement of Free-Standing Square-Millimeter Single-Layer Graphene. *Nat. Commun.* **2018**, *9*, No. 4185.
- (49) Huhtamäki, T.; Tian, X.; Korhonen, J. T.; Ras, R. H. Surface-Wetting Characterization using Contact-Angle Measurements. *Nat. Protoc.* **2018**, *13*, 1521–1538.
- (50) Tang, S.; Liu, M. R.; Lu, P.; Xia, H.; Li, M.; Xie, Z. Q.; Shen, F. Z.; Gu, C.; Wang, H. P.; Yang, B.; Ma, Y. G. A Molecular Glass for Deep-Blue Organic Light-Emitting Diodes Comprising a 9, 9'-Spirobifluorene Core and Peripheral Carbazole Groups. Adv. Funct. Mater. 2007, 17, 2869–2877.
- (51) Lim, E.; Glaudell, A. M.; Miller, R.; Chabinyc, M. L. The Role of Ordering on the Thermoelectric Properties of Blends of Regioregular and Regiorandom Poly (3-Hexylthiophene). *Adv. Electron. Mater.* **2019**, *5*, No. 1800915.
- (52) Hofstetter, Y. J.; Vaynzof, Y. Quantifying the Damage Induced by X-ray Photoelectron Spectroscopy Depth Profiling of Organic Conjugated Polymers. *ACS Appl. Polym. Mater.* **2019**, *1*, 1372–1381.
- (53) Barbey, R.; Laporte, V.; Alnabulsi, S.; Klok, H. A. Postpolymerization Modification of Poly (Glycidyl Methacrylate) Brushes: An XPS Depth-Profiling Study. *Macromolecules*, **2013**, *46*, 6151–6158.

Title: Acid-Sensitive Molecular Glasses as Removable Thin-Film Protective Layers

Table of Contents

